International Journal for Housing Science and Its Applications
Publish August 10, 2025. Volume 46, Issue 4 Pages 3959-3977

https://doi.org/10.70517/ijhsa464515a

Design Optimization of Underground Environment Monitoring System and Gas Early Warning Function Research in Extra-long Tunnels

Lingchen Meng[1,*] and Yujia Liu[2]
[1] Civil and Architectural Engineering Institute, CCCC-FHEB CO., LTD, Beijing, 100011, China
[2] Environmental Construction Ecological Restoration (Beijing) Co., Ltd, Beijing, 100011, China
Corresponding authors: (e-mail: tmjsyjymlc@163.com).

Abstract The special environment in the extra-long tunnels leads to safety accidents that are very easy to occur, and the traditional tunnel management mode has low degree of intelligence, which is not able to actively find the abnormal events in the tunnel and deal with them at the first time. For this reason, this paper proposes a kind of underground environment intelligent monitoring system, which is mainly applied to the real-time monitoring of tunnel bed settlement and deformation and gas concentration. In this system, the polar coordinate method of total station is used to obtain the three coordinates of different points, which is combined with multiple difference accuracy analysis to improve the accuracy of tunnel settlement and deformation monitoring. Based on the ARIMA model, a gas concentration prediction model is constructed, and different warning thresholds for gas concentration are set to realize the graded warning of gas in long tunnels. When monitoring the settlement and deformation of the roadbed, the deviation of the X, Y and H coordinates of each measuring station and the center error are within 1mm, and the difference between the automatic monitoring data and the manual review results fluctuates around ±0.01mm. When the ARIMA model is used to predict the gas concentration, the prediction error between the predicted value and the expected value fluctuates between ±0.05%, and a graded warning of gas concentration can be realized according to the confidence interval. The introduction of intelligent monitoring system in the underground environment of extra-long tunnels helps to optimize the tunnel construction plan and ensure the safety of extra-long tunnel construction.

Index Terms roadbed settlement and deformation, extra-long tunnel, ARIMA model, polar coordinate method, multiple difference technique

I. Introduction

With the development of transportation, the construction of highway tunnels is becoming more and more common, highway tunnels, as an important transportation infrastructure, provide convenience for people's travel, but also put forward higher requirements for the environment and safety [1]-[3]. In order to ensure the safety and environmental protection of highway tunnels, it is necessary to establish a set of perfect environmental monitoring and control system to monitor and control the environmental parameters inside and outside the tunnel in real time, so as to find out the problems in time and take measures to deal with them. Therefore, the design optimization of tunnel environmental monitoring system is particularly important [4]-[7]. The design of tunnel environmental monitoring and control system is the key to ensure the air quality and environmental safety in tunnels. A scientific and reasonable monitoring system can discover the environmental problems in the tunnel in time, and the control system can effectively control the environmental problems by automatic or manual means, especially the gas warning in the tunnel [8]-[11].

During tunnel excavation, gas concentration has a great impact on construction safety. In the case of sufficient oxygen, when the methane concentration reaches the range of 5% to 16%, there is a danger of explosion, and gas monitoring and the establishment of emergency plans are very important [12]-[15]. Tunnel excavation to take drilling and blasting method, easy to cause gas surge in the surrounding rock, in the unsupported parts of the easy formation of gas accumulation. In order to avoid the occurrence of emergencies, the design optimization of the tunnel underground environmental monitoring system is particularly important [16]-[19]. In the future, with the continuous development of technology, the tunnel environmental monitoring and control system will be improved and upgraded to adapt to more complex and diversified application environments [20], [21].

This paper proposes an intelligent monitoring system for underground environment of extra-long tunnels, which realizes real-time transmission of monitoring data through GPRS+LORA. The total station polar coordinate method

and multiple differential accuracy analysis technology are introduced to optimize the tunnel settlement and deformation monitoring data, and the gas prediction and warning model is constructed by ARIMA model.

With the continuous development of the transportation industry, tens of kilometers of extra-long tunnels continue to appear, which brings transportation convenience at the same time, the safety problem is also constantly highlighted. In order to better ensure the construction safety of the underground environment of the extra-long tunnels, this paper constructs an intelligent monitoring system applied to real-time monitoring of the underground environment. The polar coordinate method of total station system is introduced to obtain the settlement and deformation data of tunnel bed, and the data are optimized by multiple difference accuracy analysis technology to ensure the accuracy of the settlement and deformation data of tunnel bed. The gas concentration prediction model of long tunnels is established by combining the ARIMA model, and the graded warning of gas concentration in the underground environment of long tunnels is realized by setting the warning threshold of gas concentration. For the effectiveness of the system in this paper, the GQ tunnel is used as an example to carry out data validation.

II. Design of subsurface environmental monitoring systems

At present, with the acceleration of urbanization and the increase in people's concern for travel convenience, tunnels, as an important part of transportation, are becoming more and more important. However, during the construction process, tunnels may be affected by various factors and deformation may occur as well as gas leakage. In order to detect and deal with changes in the underground environment of tunnels in a timely manner, it is necessary to introduce an automated underground environment monitoring system. Automated underground environment monitoring system is a kind of continuous, real-time, automated observation, recording, analysis and early warning system for the target monitoring object by integrating all kinds of sensors, data collection and processing equipment. It can monitor the tunnel axial displacement, tunnel settlement and changes in the surrounding environment in real time, providing a guarantee for the safe operation of very long tunnels.

II. A. Overall system architecture

II. A. 1) System architecture design

Intelligent monitoring and early warning of the underground environment of long tunnels involves changes in geological conditions, the state of stress and strain in the surrounding rock and the amount of deformation, the state of the pre-reinforcement and support structure, the state of the construction environment, construction activities, etc. The basic architecture of the system is shown in Figure 1. Based on the principle of “comprehensive perception, data centralization, intelligent early warning”, this paper proposes the basic architecture of the intelligent monitoring and early warning system for the underground environment of long tunnels as shown in Fig. 1, which mainly consists of three parts: the monitoring system, the data system, and the early warning system [22]. A variety of monitoring subsystems are used to collect real-time safety index data of the underground environment of the extra-long tunnel, and the data are centralized processed and stored using the transmission network to form a data management system. Then based on the monitoring data were established deformation, environment and other advance warning model, used for tunnel construction hidden danger prediction and early disposal.

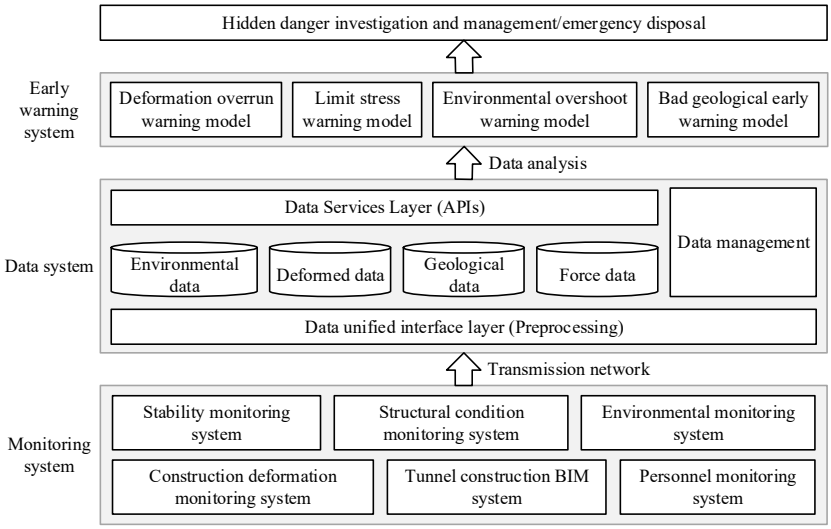

Figure 1: Underground environmental monitoring system architecture

The selection of the monitoring system is based on the principles of “flexibility, reliability, durability and economy”, which can adapt to the requirements of long-distance construction monitoring of long tunnels, can be measured flexibly and is easy to install and dismantle, with low cost of use, high reliability and long service life in complex operating environments. The monitoring points should be reasonably arranged in combination with the site conditions, and the monitoring scope should cover all dangerous work surfaces, and the quantity, frequency and quality of the monitoring data should meet the requirements for analysis and prediction. Priority should be given to wireless transmission technologies such as WIFI, Bluetooth, Zigbee, 4G/5G, etc., to realize interconnection between sensors or measuring devices, long-distance data collection and centralized processing.

II. A. 2) System monitoring process

According to the actual application effect, the comprehensive application effect of automated monitoring technology far exceeds that of traditional monitoring technology in terms of enhancing the timeliness of monitoring results and reducing operational burden. From the perspective of timeliness of monitoring results, under the traditional monitoring mode, the monitoring personnel manually read, record and summarize a large amount of monitoring data, the monitoring process is cumbersome, and the monitoring report only describes the construction process in the past period of time. The application of automated monitoring technology can simplify the process steps, shorten the monitoring data processing time, and synchronize the update of monitoring reports and charts. The automated monitoring process of underground environment of long tunnels is shown in Figure 2, which mainly includes six links of system deployment, program design, point placement, data processing, manual review, warning and alarm.

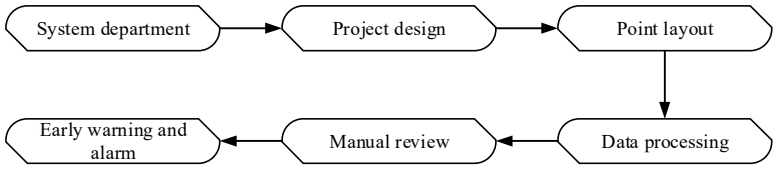

Figure 2: Monitoring process for underground environment automation

(1) System deployment. Automatic monitoring system consists of hardware and software facilities, around the tunnel underground environmental monitoring task requirements, do a good job of facility selection.

(2) Program design. Tunnel engineering site space is narrow, monitoring accuracy requirements are strict, the monitor can take measurement robotics, combined with engineering conditions, the development of deformation monitoring, tunnel convergence monitoring, gas early warning and other items of special monitoring programs.

(3) Point Layout. Benchmark points, monitoring section to monitoring points as the content of the layout, comprehensive analysis of the monitoring project and construction site environment, clear the specific location of all the points, many measurement points together to form a monitoring section, accurately describing the changes in the state of the tunnel structure.

(4) Data processing. In the case of constructing the monitoring network only from the reference point, or from the reference point, monitoring points together constitute the monitoring network, the real-time measurement data and historical measurement data as a test basis, calculate the difference between the measurement data before and after. Using a combination of comparative method to judge, in order to compare the error in the weight of the unit of measurement before and after, check the change in the displacement of the reference point as the basic idea, to find out the change of the reference point.

(5) Manual review. Due to the complex environment of the tunnel site, the automated deformation monitoring results will produce a certain degree of error, so it is necessary to manually review all the observation points to the roadbed settlement, gas data and other monitoring results as the review content.

(6) Early warning and alarm. Set the upper and lower limits of each parameter in the automated monitoring system, the system compares the measured values with the limits by itself, and if the measured value is lower than the lower limit or exceeds the upper limit, the alarm program will be started immediately to remind the monitoring personnel and the engineering construction units.

II. B.System function realization

II. B. 1) Database design

The database management system used in this system is SQL Server, and the database is designed into two levels, i.e., the central management database and the hierarchical project database, to meet the needs of the database for the management of different projects and project data and information. The center management database is used to manage the basic information of all projects, and each project corresponds to a project database, including all

the configuration information and monitoring information of the project. The database design mainly consists of project table, user information table, and abnormal login information table. The project database is used to manage the configuration information as well as monitoring data and results of each project, and the designed data table mainly contains the configuration information and monitoring data information of the project.

II. B. 2) Early warning program design

Designing the wireless sensor network program for the data acquisition subsystem in the underground environment monitoring system of the extra-long tunnel, this paper takes the GPRS network and LORA technology as the basis, and designs the gas early warning program in consideration of the actual situation of the tunnel construction work surface and air flow and other factors. The specific scheme is that LORA sensing node collects environmental data such as carbon monoxide, methane and gas in the tunnel, and sends the data to the GPRS-LORA convergence node in the area; the GPRS base station sends the converged data to the tunnel monitoring server for the monitor to watch through GPRS, with the help of mobile Internet.

Gas concentration monitoring through the underground environment monitoring system, which can be based on different gas concentrations for real-time monitoring, if the monitoring gas exceeds the set alarm value, the operation site will sound and light alarm, the monitoring center will also receive alarm prompts. The gas alarm controller can be connected to multiple monitoring points at the same time, and display the data of multiple gas monitors on one machine. When a fixed point of the gas detector alarm, the controller can accurately display and lock the alarm location in time to investigate and solve the problem of excessive gas concentration at the alarm location.

III. Tunnel settlement deformation and gas early warning technology

With the continuous promotion of underground space development, more and more underground projects are close to established structures such as tunnels, which require effective and real-time protective monitoring of underground tunnels during the construction process. Total station is a high-precision, high-reliability, three-dimensional measurement, remote control of the measurement means, has been widely used in the long tunnels underground environment of automated monitoring projects. In order to effectively realize the effective monitoring of the underground environment of long tunnels, this chapter mainly introduces the deformation displacement and gas prediction and early warning technology in the tunnel construction process, aiming to improve the intelligent monitoring effect of the underground environment of long tunnels, and better ensure the construction safety of long tunnels.

III. A. Tunnel settlement and deformation monitoring

III. A. 1) Principles of deformation monitoring

The total station system is a three-dimensional coordinate measurement system of photoelectric ranging and electronic angular measurement. After accurately measuring the edge and angle relationship between the monitoring point and the reference point, the elevation and plane coordinates of the monitoring point are accurately deduced based on the edge and angle relationship.

The known information is the elevation and coordinates of the reference point A,B,C, the set mirror point of the intelligent total station is P, and the monitoring point is i. Using the principle of backward rendezvous measurement, the elevation and coordinates of the point P are calculated (XP, YP, HP), and then the coordinates and elevation of the monitoring point i are deduced (X_P,Y_P,H_P) [23]. If the initial value is set to the coordinate value of the first cycle of the monitoring point, i.e., (X_i,Y_i,H_i), the relative value of the deformation of the other monitoring points in the n th period and the first cycle is:

$$\Delta X = X_i^n - X_i^1 \tag{1}$$

$$\Delta Y = Y_i^n - Y_i^1 \tag{2}$$

$$\Delta H = H_i^n - H_i^1 \tag{3}$$

III. A. 2) Polar-coordinate deformation monitoring

The automatic tunnel monitoring method based on intelligent total station is to set up reference points at both ends of the tunnel, calculate the coordinates of the intelligent total station placed at the survey site by aiming at multiple known reference points using the free station setting method, and then observe the three-dimensional coordinates of the monitoring points in multiple monitoring sections using the polar coordinate measurement method.

The free station method is a measurement method that places a total station on the measuring station and observes the directions and distances of several known datums, and calculates the coordinates of the measuring station according to the indirect leveling method. Indirect leveling takes the coordinates of the survey station to be determined as the unknown parameters, establishes the corresponding error equations according to various types of observations, and then calculates the coordinate leveling value of the survey station based on the principle of least squares. When using the free station method to calculate the coordinates of the survey station, the plane and elevation coordinates can be leveled separately, while a more rigorous leveling model takes the slope distance, horizontal direction and zenith distance as the original observation values, and the three-dimensional coordinates of the survey station as the unknown parameters for leveling [24].

In the establishment of the coordinate system for tunnel monitoring, the X-axis of the coordinate system is generally selected to be along the longitudinal direction of the tunnel, and the Z-axis is along the plumb direction. At this time, the change of the Y-axis of the monitoring point of each monitoring section is the deformation of the tunnel in the radial direction, and the change of the Z-axis is the settlement of the tunnel arch or the tunnel floor.

After obtaining the three-dimensional coordinates of the survey station through the free station setting method, the coordinates of each monitoring point can be obtained through the polar coordinate method. The specific calculation formula is:

$$\left.\begin{aligned} X_P &= X + S_P \sin A_P cos(w + L_P) \\ Y_P &= Y + S_P \sin A_P sin(w + L_P) \\ Z_P &= Z + S_P cos A_P \end{aligned}\right\} \tag{4}$$

where (X_p, Y_p, Z_p) is the coordinate of the monitoring point, (x, y, z) is the coordinate of the measuring station, S_P is the observed value of slant distance, A_P is the observed value of zenith distance, L_P is the observed value of horizontal direction, and w is the orientation angle.

During the monitoring process, since the intelligent total station adopts forced centering and the target prism is always fixed on the tunnel section, the centering error and target eccentricity error can not be considered. According to the law of error propagation, the accuracy of the coordinates of monitoring point P in each direction can be obtained as follows:

$$\begin{aligned} m_{X_P}^2 &= m_X^2 + m_S^2 (\sin A_P \cos(w + L_P))^2 \\ &+ m_A^2 (\cos A_P \cos(w + L_P))^2 \frac{S_P^2}{\rho^2} + (m_L^2 + m_w^2) \\ &+ (\sin A_P \sin(w + L_P))^2 \frac{S_P^2}{\rho^2} \end{aligned} \tag{5}$$

$$\begin{aligned} m_{Yp}^2 &= m_Y^2 + m_S^2 (\sin A_P \sin(w + L_P))^2 \\ &+ m_A^2 (\cos A_P \sin(w + L_P))^2 \frac{S_P^2}{\rho^2} \\ &+ (m_L^2 + m_w^2) + (\sin A_P cos(w + L_P))^2 \frac{S_P^2}{\rho^2} \end{aligned} \tag{6}$$

$$m_{Z_P}^2 = m_Z^2 + m_S^2 \cos A_P^2 + m_A^2 (\sin A_P^2) \cdot \frac{S_P^2}{\rho^2} \tag{7}$$

where m_X, m_Y, m_Z is the median error of each direction of the station, m_w is the median error of the orientation angle, and m_S, m_A, m_L is the median error of the oblique distance, zenith distance, and the horizontal observation, respectively. m_X, m_Y, m_Z, m_W can be calculated according to the free station setting, m_S, m_A, m_L can be obtained from the nominal accuracy of the observation instrument.

III. A. 3) Multi-differential accuracy analysis

In order to further improve the accuracy of 3D coordinate data obtained by total station, this paper introduces multiple real-time differential correction for accuracy analysis, with a view to providing accurate data support for the study of tunnel deformation and settlement displacement. The differential correction technique is to take the

observation difference of a specific datum as the data correction standard of the target monitoring point [25]. Then there is a precondition that the measurement site and the reference point must be in an absolutely stable state, assuming that all the error effects except for the errors generated by meteorological factors are eliminated. In order to weaken the impact of polar coordinate measurement errors and improve the measurement accuracy, multiple real-time differential correction techniques can be used.

(1) Differential correction of slant distance

If the known slant distance from the station to a reference point is S_f^0 (or the initial value of the slant distance) and the measured slant distance for a certain period is $S_J^{'}$, and the difference between it and the known slant distance can be considered to be caused by a meteorological element, the proportionality correction factor for the slant distance, ΔS, can be obtained:

$$\Delta S = \frac{S_J^{'} - S_J^{'}}{S_J^{'}} \tag{8}$$

If the slant distance of a deformation point P point measured in cycle n is S_J^n, then the differential corrected distance of the point is:

$$S_P = S_J^n + \Delta S \cdot S_J^n \tag{9}$$

(2) Differential correction of elevation difference

Differential correction of elevation difference is to assign the difference of elevation difference of datum to each monitoring point for elevation value correction. Assuming that the elevation difference between a measured station and a reference point is h_J, then there is:

$$h_J = S_J \sin\alpha + i_J - \partial_J \tag{10}$$

where α is the vertical angle, i_J is the instrument height, and $\hat{\sigma}_J$ is the prism height. Then the height difference correction factor c is:

$$c = \frac{\Delta h^0 - h_J}{S_J^2 \cos^2\alpha} \tag{11}$$

where Δh^0 is the known elevation difference between the station and the reference point, and its value can be obtained by high-grade level measurement.

After obtaining the elevation correction coefficient through the above formula, it can be concluded that the differential corrected elevation difference of the deformed point is:

$$\Delta h_p = S_P \sin\alpha + cS_p^2 \cos^2\alpha + i_J - \partial_J \tag{12}$$

After finding the slope distance and elevation difference of the deformed point after correction, then the flat distance after differential correction can be found as:

$$D_p = \sqrt{S_p^{\ 2} - \Delta h_p^{\ 2}} \tag{13}$$

(3) Differential correction of azimuth angle

The azimuth H_{ZJ}^0 acquired at the initial measurement of the reference point is taken as the reference azimuth, and the azimuth $H_{zJ}^{'}$ measured at the reference point in other cycles is compared with the reference azimuth to obtain a difference ΔH_z as:

$$\Delta H_z = H_{zJ}^{'} - H_{zJ}^0 \tag{14}$$

According to the principle of difference, take the correction value ΔH_z of the reference point as the basis standard, and add this correction value to the measured angle value $H_{ZP}^{'}$ of each deformation point in real time, so as to accurately derive the azimuth angle H_{ZP} of each deformation point after differential correction:

$$H_{ZP} = H_{ZP}^{'} - \Delta H_Z \tag{15}$$

(4) Calculation of three-dimensional coordinates of deformation points and deformation amount

After the slope distance, height difference and azimuth difference correction, the three-dimensional coordinates of each deformation point can be calculated as:

$$\begin{cases} X_P = D_P \cos H_{ZP} + X^0 \\ Y_P = D_P \sin H_{ZP} + Y^0 \\ Z_P = \Delta h_P + Z^0 \end{cases} \tag{16}$$

where X^0, Y^0, Z^0 is the three-dimensional coordinate value of the measuring station.

If the coordinate value (X_p^1, Y_p^1, Z_p^1) of the first cycle of the deformation point is used as the initial value, then the cumulative deformation of each deformation point relative to the first cycle is:

$$\begin{cases} \Delta X_P = X_P - X_P^1 \\ \Delta Y_P = Y_P - Y_P^1 \\ \Delta Z_P = Z_P - Z_P^1 \end{cases} \tag{17}$$

Differentiating both sides of Eq. (16) and converting to the form of the median error, the accuracy estimation formula for polar coordinate differential 3D measurement can be obtained as:

$$\begin{cases} m_{X_p}^2 = \cos^2 H_{2P} \cdot m_{D_p}^2 + D_P^2 \cdot \sin^2 H_{ZP} \cdot \left(\dfrac{m_{H_{PP}}}{\rho} \right)^2 \\ m_{Y_p}^2 = \sin^2 H_{ZP} \cdot m_{D_p}^2 + D_P^2 \cdot \cos^2 H_{ZP} \cdot \left(\dfrac{m_{H_{PP}}}{\rho} \right)^2 \\ m_{ZP}^2 = m_{\Delta h_P}^2 \end{cases} \tag{18}$$

According to the Helmert point error estimation equation, i.e:

$$m_P = \pm \sqrt{m_x^2 + m_y^2 + m_z^2} \tag{19}$$

Substituting Eq. (18) into Eq. (19) yields the point median error at point P as:

$$m_p = \pm \sqrt{m_{D_p}^2 + \left(\frac{D_p}{\dot{\rho}} \right)^2 m_{Hzp}^2 + m_{\Delta h_p}^2} \tag{20}$$

where m_{D_p} is the median error of the flat distance D_p between the station and the deformed point, and $m_{\Delta h_p}$ is the median error of the corrected height difference Δh_p between the station and the deformed point.

III. B. Early warning for gas concentration prediction

III. B. 1) ARIMA model

Autoregressive sliding average modeling (ARIMA) is a typical method for studying the rational spectrum of smooth stochastic processes and is applicable to a large class of practical problems [26]. The data series formed by the predictive indicators over time is regarded as a random sequence, and the dependence that this group of random variables has reflects the continuity of the original data in time. On the one hand, the influence of influencing factors, on the other hand, has its own pattern of change.

Assuming that the influencing factor is $x_1, x_2, ..., x_k$, it can be obtained by regression analysis:

$$Y_t = \beta_1 x_1 + \beta_2 x_2 + ... + \beta_p x_p + Z \tag{21}$$

where Y is the observed value of the prediction object and Z is the error. As the prediction object Y_t is affected by its own changes, its law can be expressed as:

$$Y_t = \beta_1 Y_{t-1} + \beta_2 Y_{t-2} + ... + \beta_p Y_{t-p} + Z_t \tag{22}$$

The error term has a dependence across time, then:

$$Z_t = \varepsilon_t + \alpha_1 \varepsilon_{t-1} + \alpha_2 \varepsilon_{t-2} + ... + \alpha_q \varepsilon_{t-q} \tag{23}$$

From this, the ARIMA model expression is obtained as:

$$Y_t = \beta_0 + \beta_1 Y_{t-1} + \beta_2 Y_{t-2} + ... + \beta_p Y_{t-} p + \varepsilon_t + \alpha_1 \varepsilon_{-1} + \alpha_2 \varepsilon_{t-2} + ... + \alpha_q \varepsilon_{t-q} \tag{24}$$

III. B. 2) Forecasting models and processes

The prediction and early warning of gas concentration in underground environment monitoring point of special long tunnels take the real-time monitoring data of underground single monitoring point gas as the object of analysis, through the pre-processing of real-time monitoring data of gas, based on the calculation principle and method of ARIMA model, establish the prediction model of gas concentration in a single monitoring point to get the prediction interval, and carry out the early warning analysis based on the prediction result. The detailed flow of this prediction and warning method is shown in Figure 3, and the specific calculation steps are as follows:

(1) Gas monitoring data preprocessing. Abnormal data processing and missing data processing are carried out sequentially on the collected real-time gas monitoring data.

(2) Initialize the model order and forward prediction step.

(3) Determination of modeling sample length.The determination of the sample length of ARIMA gas concentration prediction model, theoretically, through the time series analysis, can choose the inverse of the inverse of the two adjacent frequency intervals in the time series frequency domain as the integer multiple of its length.

(4) Zero-mean processing of monitoring data. As in the preprocessing stage, the mean value μ_x of time series $\{x_t, t = 1, 2, \cdots, N_x\}$ is first calculated and then processed using the following equation, i.e.:

$$x'_t = x_t - \mu_x, t = 1, 2, \cdots, N_x \tag{25}$$

At the same time, normalization is required in order to reduce rounding errors and avoid overflow, i.e:

$$\chi'_t = (x_t - \mu_x) / \sigma_x \tag{26}$$

where σ_x is the variance of the time series $\{x_t, t = 1, 2, \cdots, N_x\}$, and again after obtaining the final prediction $\hat{x}_t$, the inverse normalization, i.e., the mean needs to be restored to give the prediction approximation multiplied by the sample variance plus the mean μ_x:

$$x_t = \hat{x}_t \sigma_x + \mu_x \tag{27}$$

(5) Model parameter estimation. Based on the basic principles of ARIMA method, the model parameters are estimated using the least squares method in ARIMA model parameter estimation method.

(6) Model testing and order setting. The method in (5) is used to estimate the model parameters, and the information criterion AIC method is used to determine the suitable model and its order p.

(7) Gas concentration prediction. The prediction interval $PA = [\delta_{1j}, \delta_{2j}], j = 1, 2, \cdots, np$ is obtained by successive forward np-step prediction calculations, where the prediction interval of gas concentration is the upper and lower envelopes of the predicted values, and the upper and lower displacements are the product of the quantile of the posterior probability distribution of the predicted sample and the open square of its variance at a given confidence level. According to the nature of Gaussian distribution, the prediction interval is expressed as:

$$PA = [m(\dot{y}) - \beta\sqrt{\mathrm{cov}(\dot{y})}, m(\dot{y}) + \beta\sqrt{\mathrm{cov}(\dot{y})}] \tag{28}$$

where $cov(\hat{y})$ is the variance of the model estimate, β is the quantile of the posterior probability distribution of the sample data at a given confidence level, and β is generally taken as 95% to ensure the validity of the prediction interval.

(8) Calculate the best revised prediction results. Calculate the best prediction result and its corresponding prediction interval according to the dynamic correction method.

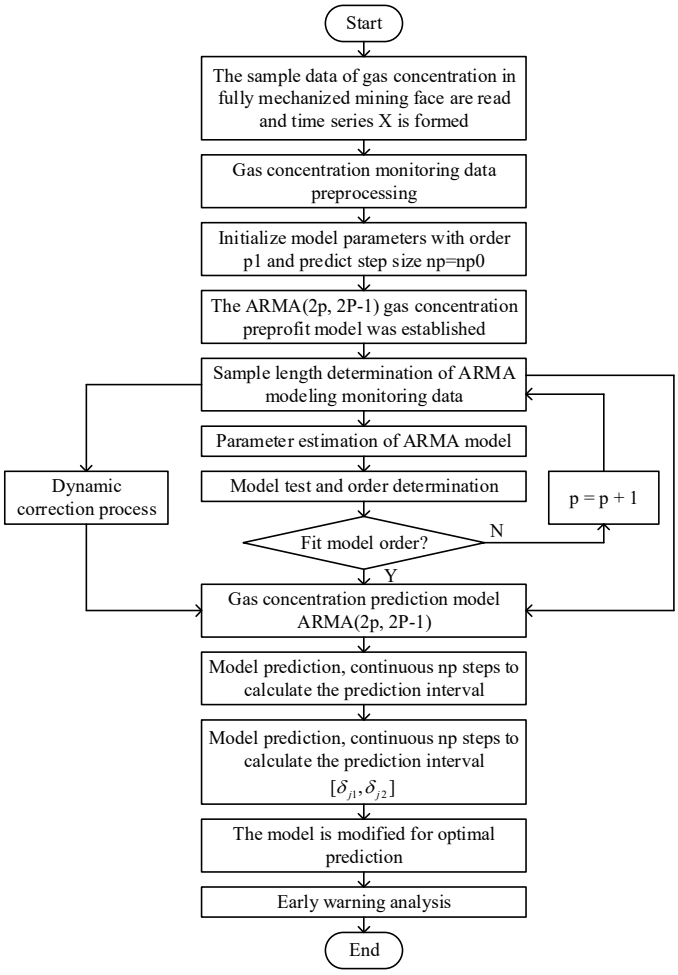

Figure 3: Gas concentration forecast model flowchart

III. B. 3) Gas concentration warning thresholds

Based on the above method of analyzing gas concentration anomalies at monitoring points, and on the premise of calculating the predicted value of gas concentration and the prediction interval. If the alarm concentration of gas concentration at a certain type of monitoring point stipulated in the regulations is w_s, the following method is used to determine the warning threshold of gas concentration at the monitoring point and to classify the warning level.

(1) Level I warning. If the predicted value of gas concentration and the upper boundary of the prediction interval $x \cdot + \delta \cdot \le \mu_x + \sigma_x$, that is, when the predicted value falls within the 68.3% confidence interval of the gas concentration time series, it is regarded as a normal situation and no warning alert is made. Under the premise of $x^* < w_2$, when $x^* + \delta^* \in [\mu_x + \sigma_x, \mu_x + 1.44_{\sigma x}]$, i.e., the predicted value falls within the 85% confidence interval of the gas concentration time series, it is regarded as a normal situation and no warning alert is made, and vice versa, it is regarded as the gas concentration is large. Calculate the time when the predicted value of gas concentration is consistently large for 1 hour in a row t_h, when $t_h > 30\,\min$, if $\mu_r < \mu_r$, it indicates that the sample to which the predicted value belongs is weakly correlated with other sample data. And the predicted value of gas concentration has a tendency to continue to be large, which is an abnormal situation, and is designated as warning level I. Use t_w to indicate the warning time, set the warning time $t_h \le t_w \le 1h$, if $\mu_{r'} \ge \mu_r$, indicating that the predicted value belongs to the sample and other samples of data correlation is strong, as a normal situation, do not do warning warning.

(2) Early warning level II. When $x^* + \delta_2 \in (\mu_x + 1.44\sigma_x, \mu_x + 1.96\sigma]$, the abnormal situation is analyzed according to the method in (1), and conversely, when $x + \delta_2 > \mu_x + 1.96\sigma_x, x^* < w_z$, i.e., when the gas concentration does not reach the alarm threshold value, the time of sustained large gas concentration prediction in 1 consecutive hour is calculated t_h. If $t_h > 30\,\min$, and $\mu_r < \mu_r$, i.e., the predicted value falls between the 85%~95% confidence intervals of the time series of the gas concentration, the predicted value of the gas concentration has a trend of sustained

large gas concentration. And the sample to which the predicted value belongs has a weak correlation with other gas concentration samples, then it is an anomaly and is set as Alert Level II. If alert time $t_h \le t_w \le 1h$ is set, and if $\mu_r \ge \mu_r$ is set, then the predicted gas concentration value has a persistent large trend, but the sample to which the predicted value belongs has a strong correlation with other samples, and it is designated as alert level I.

(3) Early warning level III. When $x+\delta_2 > \mu_x + 1.96\sigma_x, x^* < w_z$, i.e., the gas concentration does not reach the alarm threshold value, calculate the time of continuous excursion t_h within 2 hours. If $t_h > 60\min$, and $\mu_r < \mu_r$, i.e., the predicted value has not yet exceeded the alarm concentration, but it does not fall within the 95% confidence interval of the gas concentration time series, and there is a persistent tendency for the predicted value of the gas concentration to be large. And the samples to which the predicted value belongs are weakly correlated with other gas concentration samples, which is designated as warning level II, and the warning time is set at $t_h \le t_w \le 2h$. If $\mu_{r'} \ge \mu_r$, it indicates that the predicted value of gas concentration has a tendency to continue to be large for a longer period of time. However, the sample to which the predicted value belongs has a strong correlation with other sample data, and is designated as early warning level II. If it is $30\min < t_h < 60\min$ or $\mu_r < \mu_r$, it will be designated as early warning level II, otherwise it will be designated as early warning level I.

For the application of gas early warning analysis in the underground environment of long tunnels, the threshold value of the basic warning indicators can be set according to the actual situation of the underground environment of long tunnels to set suitable confidence intervals, and analyze the gas concentration anomalies in combination with the warning indicators to classify the warning level.

IV. Examples of Tunnel Settlement and Deformation and Gas Early Warning

Urban development makes transportation more convenient, and the construction process of long tunnels will cause changes in the surrounding infrastructure, and the possible existence of gas leakage for the construction of tunnels to bring greater safety hazards. Based on this, it is necessary to use an automated underground environment monitoring system to monitor the underground environment of long tunnels in real time. In this paper, an automatic underground environment monitoring system is designed for long tunnels, and this chapter mainly quantitatively analyzes the effect of tunnel deformation and settlement, gas monitoring and early warning, in order to provide a guarantee for the construction safety of long tunnels.

IV. A. Overview of the project and location of points

IV. A. 1) Summary of works

XC Railway GQ Tunnel is located in XH County Ganjia Township - Tongren County Shuangpengxi Township, for the Qinling Mountains in the alpine landscape, is a plateau continental climate, low temperatures, large temperature difference between day and night, strong sunshine, long freezing period. Average annual precipitation 465.6mm, precipitation is concentrated in April to September, the maximum precipitation of 598.4mm, the average annual evaporation of 1379.8mm, the amount of water with the seasonal changes in the larger, no large river development, the overall distribution of the trend of the south and north of the distribution of high and low, the vegetation is more lush.

GQ tunnel is a single-hole, two-lane combined tunnel, tunnel start and end mileage DK378+056~DK405+427, the total length of 24.57km, the tunnel inlet elevation is 3251.24m, the exit elevation is 2,747.85m, the tunnel maximum depth of 680m, the relative difference in elevation 220~640m. Tunnel inlet traffic is more convenient, site conditions are better, the tunnel exit, the exit of the local level guide traffic is more difficult, the construction site conditions are better. 1 inclined shaft, No. 2 inclined shaft, No. 3 inclined shaft traffic is convenient, site conditions are better, the No. 4 inclined shaft traffic is more convenient, site conditions are worse.

The tunnel is located in the middle and high mountainous areas, exposed bedrock, the tunnel body is mainly Yanshan period amphibolite and tectonic rocks, the tunnel peripheral rock is mainly Ⅳ, Ⅴ peripheral rock, there is no large-scale river area, the gully in the region is deeper, subject to geological and tectonic movements, fracture structure development, large gully with multi-year running water. The tunnel is located in the Ganjia Basin, Guashizhe Basin location, mostly grasslands and pastoral areas, the slope of the hill is more comfortable.

IV. A. 2) Placement of points

(1) Laying of reference points. Benchmark points should be distributed on both sides of the construction site and outside the safety, stability and construction influence range. They shall be calibrated periodically to prevent errors caused by their own variations. The datum points shall be laid according to the following 3 points, viz:

The distance between the datum point and the measurement point should be within 100m to maintain good visibility and ensure high precision measurement results. The datum point should be buried in hard soil and high

water table to ensure the stability of the datum point itself. The datum is drilled with a drilling rig, pre-buried with steel bars and poured with concrete for vibration compaction. A protection well is built around it, and a steel protection cover is installed on the top.

(2) Laying of working points. The working base point is completed buried by forming a hole in the soil of manual excavation or drilling tools. The whole laying process is as follows:

Use Luoyang shovel to excavate the soil surface manually or use Φ90mm drilling tool to excavate the harder surface to a diameter of 90mm and a depth of more than 3.5 m. Compact the bottom, clean the soil, and pour a small amount of water into the tunnel for maintenance. Pour cement of grade not less than C25 and use vibrating equipment to make it dense, ensuring that the top of the cement is within 6cm of the ground. Place rebar markers with a diameter of not less than 90cm inside the hole, exposing the concrete surface for about 2~3cm. install a steel protective cover on the upper part and maintain it for more than 20d.

(3) Deformation monitoring point layout. Deformation monitoring point layout in line with the requirements of the new project, monitoring point layout in the original project relative to the scope of the fall every 12m set up. Each monitoring section consists of 1 tunnel arch settlement point, 2 tunnel horizontal displacement points and 2 track vertical displacement monitoring points, a total of 30 sections.

According to the requirements of the technical program and relevant specifications and combined with the actual situation of the project, the monitoring cycle is to continue monitoring for more than 4 months after the completion of the pit construction and to end the monitoring work when the settlement rate is less than ±0.05mm/d in the last 90 days. The automated monitoring work was carried out from June 1, 2023 to June 5, 2023 to collect the initial value, and from the first monitoring on June 6, 2023 to December 16, 2023, a total of 203 days of monitoring. Throughout the monitoring cycle, both the upstream and downstream lines were monitored at a frequency of once every three hours for a total of eight times per day.

IV. B. Tunnel deformation and settlement monitoring

IV. B. 1) System stability analysis

Before the start of external construction, the environmental state inside the tunnel is stable, which can be regarded as the position of each control point in the control network is fixed, and the automated control network joint measurement leveling is carried out continuously, and the average value of the results of five control network joint measurement leveling is taken as the true value of the coordinates of each control point in the control network. Comparing the coordinates of the five measurement robots in the control network in each period of joint measurement and the true value, the average value of the deviation of the coordinates of the points and the statistics of the error in the coordinates are shown in Table 1 and Table 2.

From the comparison statistics, it can be seen that the average value of the coordinate deviation and the error in the coordinates of each measuring station in the control network are all within 1mm, the Y coordinate deviation of the measuring stations on both sides is small, and the closer to the middle, the larger the Y coordinate deviation of the measuring stations is, and the Y coordinate deviation of the measuring station of Test3 is the largest of 0.708mm, which is mainly due to the accumulation of the error in the distance measurement in the course of the measurement of the monitoring control network, resulting in a larger Y coordinate error along the tunnel direction. The average values of the deviation of X, Y and H coordinates of each measurement site are 0.031mm, 0.424mm and -0.068mm respectively, and the average value of the deviation of the point position is 0.435mm, and the maximum error in the coordinates is 0.914mm, which is all within 1mm. This paper shows that the automated underground environment monitoring system of the long tunnel has good stability of point placement and high sensitivity of deformation monitoring, which can meet the requirements of deformation monitoring of long tunnels.

Table 1: Statistical table of deviation of measuring station coordinate

-	$\Delta X(mm)$	$\Delta Y(mm)$	$\Delta H(mm)$	$\Delta P(mm)$
Test1	0.003	0.181	-0.052	0.181
Test2	0.012	0.254	-0.103	0.284
Test3	-0.028	0.708	-0.021	0.713
Test4	0.054	0.649	-0.114	0.661
Test5	0.115	0.327	-0.048	0.335

Table 2: Statistical table of root mean square error of measuring station coordinate

-	$\sigma X(mm)$	$\sigma Y(mm)$	$\sigma H(mm)$	$\sigma P(mm)$
Test1	0.051	0.287	0.115	0.321
Test2	0.004	0.358	0.162	0.393
Test3	0.062	0.903	0.137	0.914
Test4	0.083	0.852	0.222	0.889
Test5	0.128	0.401	0.143	0.438

IV. B. 2) Tunnel bed settlement

During the construction process of the pit project in the extra-long tunnel, the measurement robot automated monitoring system was used to compare and analyze the overall deformation of the tunnel structure and the manual level measurement data, and the comparison results of the roadbed settlement data are shown in Fig. 4, of which Fig. 4(a)~(b) are the comparison results of the cumulative amount of settlement and the reciprocal difference of settlement, respectively.

From Fig. 4(a), it can be seen that the foundation pit caused obvious settlement impact on the tunnel bed during the construction process, and both manual and automated measurements show that the monitoring section 16 is the location of the maximum settlement, and the settlement is 25.51mm for manual measurement and 23.13mm for automated measurement, and the difference between the two errors is 2.38mm.Overall, the monitoring results of manual and automated measurements are more consistent, and the settlement trend is the same. The settlement trend is the same. Combined with Fig. 4(b), it can be seen that the mutual difference between the manual and automated measurements is within 3mm, in which the maximum mutual difference of monitoring section 11 is 3.00mm, and the overall average mutual difference of all the monitoring points is 1.243mm, which indicates that the results of the automated monitoring system of the roadbed settlement monitoring results are more consistent with the results of manual monitoring, and it can satisfy the precise monitoring of the settlement and deformation of the roadbed of the tunnel underneath the tunnel in the underground environment of the extra-long tunnels.

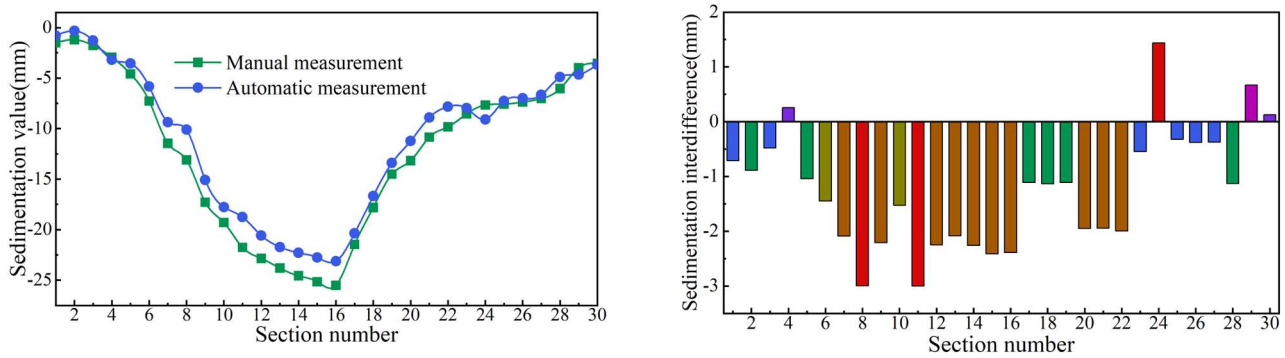

(a) Sedimentation accumulation (b) Sedimentation interdifference

Figure 4: Comparison results of the settlement data of the road bed

IV. B. 3) Monitoring of differential settlement in the roadbed

After analyzing the change trend of tunnel bed settlement, this paper further analyzes the cumulative change amount and rate of change of tunnel bed differential settlement of the upstream and downstream lines, so as to further grasp the trend of tunnel bed settlement and deformation in the underground environment of long tunnels, and to provide support for the safe construction of long tunnels.

(1) Analysis of differential settlement of the roadbed in the upstream line

Figure 5 shows the cumulative changes in differential settlement and rate of change of the upstream roadbed at different cross-section monitoring points, of which the left and right axes are the cumulative changes in differential settlement and rate of change of the roadbed in the whole monitoring cycle and the last 90 days, respectively. From the figure, it can be seen that in the whole monitoring cycle, the maximum cumulative change of monitoring point No. 6 is 0.523 mm, and the minimum cumulative change of monitoring point No. 3 is -0.815 mm. Meanwhile, the maximum and minimum values of the change rate of the two monitoring points are 0.003 mm/d, and -0.004 mm/d. In the whole monitoring cycle, in the analysis of the monitoring of bed settlement on upstream line, the maximum

and minimum values of the bed settlement on upstream line corresponding to the monitoring point No. 6 are 0.003 mm/d, -0.004 mm/d. In the whole monitoring cycle, the maximum values of cumulative change amount and change rate of upstream bed settlement corresponding to monitoring point No. 6 and the minimum values of cumulative change amount and change rate of upstream bed settlement corresponding to monitoring point No. 3 of the cross section. In the last 90 days of the monitoring cycle, the maximum cumulative change of 0.438 mm was observed at monitoring point No. 19, and the minimum cumulative change of -0.412 mm was observed at monitoring point No. 23. Meanwhile, the maximum and minimum values of the change rate of the two monitoring points were 0.005 mm/d and -0.005 mm/d, respectively.In the last 90 days of the monitoring cycle, the analysis of the upgradient roadbed settlement monitoring Maximum values of cumulative change amount and change rate of upstream roadbed settlement corresponding to monitoring point No. 19 of the cross-section occurred, and minimum values of cumulative change amount and change rate of upstream roadbed settlement corresponding to monitoring point No. 23 of the cross-section occurred.

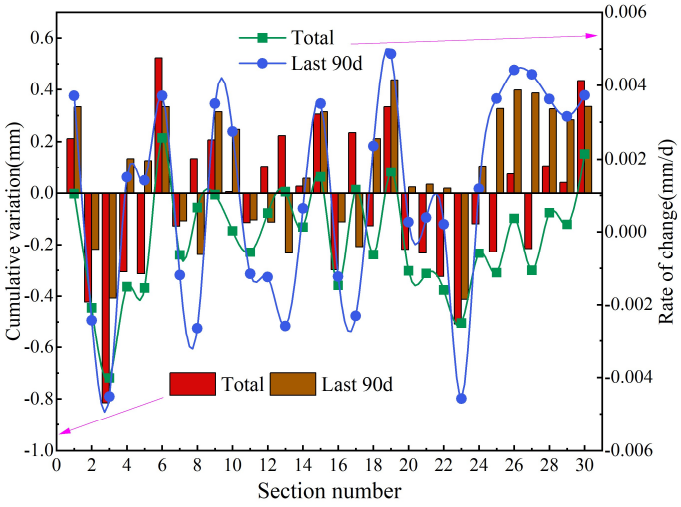

Figure 5: The difference of the line of the upper line is settled

(2) Analysis of differential settlement of downstream roadbed

Figure 6 shows the cumulative changes in differential settlement and rate of change of downstream roadbed at different monitoring points, where the left and right axes are the cumulative changes in differential settlement and rate of change of roadbed in the whole monitoring cycle and the last 90 days, respectively. As can be seen from the figure, during the whole monitoring cycle, the maximum value of cumulative change at monitoring point No. 6 of section is 0.538mm, and the minimum value of cumulative change at monitoring point No. 28 of section is -0.938mm. At the same time, the maximum and minimum values of the change rate of the two monitoring points are 0.003mm/d and -0.005mm/d. In the whole monitoring cycle, in the analysis of downstream bed settlement monitoring, the maximum values of the cumulative change of the downstream bed settlement and the change rate of the downstream bed settlement corresponding to the monitoring point No. 6 of the section, and the minimum values of the cumulative change of the downstream bed settlement and the change rate of the downstream bed settlement corresponding to the monitoring point No. 28 of the section, were observed. Minimum values occur. In the last 90 days of the monitoring cycle, the maximum cumulative change of 0.524 mm was recorded at monitoring point No. 15 and the minimum cumulative change of -0.936 mm was recorded at monitoring point No. 9. Meanwhile, the maximum and minimum values of the rate of change at the two monitoring points were 0.006 mm/d and -0.01 mm/d, respectively. In the last 90 days of the monitoring cycle, the analysis of the monitoring of the downstream roadbed settlement In the last 90 days of the monitoring cycle, the maximum values of cumulative change amount and change rate of downstream roadbed settlement corresponding to monitoring point No. 15 of the cross-section and the minimum values of cumulative change amount and change rate of downstream roadbed settlement corresponding to monitoring point No. 9 of the cross-section both appear.

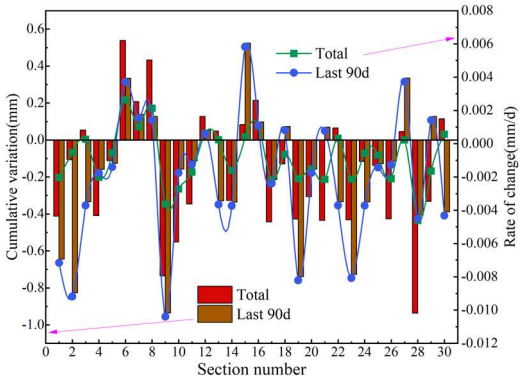

Figure 6: The difference of the line of the lower line is settled

The tunnel bed settlement was categorized into upward and downward lines, and the cumulative changes and rates of change for each monitoring point number were counted for the whole monitoring cycle and for the last 90 days. The conclusions are as follows:

(1) The overall change in the differential settlement of the roadbed in the upstream line is small, with the maximum cumulative change of -0.815mm, and the cumulative change of each monitoring point does not exceed the warning value (±1.5mm). The cumulative change is roughly distributed in wave shape along the mileage, and the cumulative change of each monitoring point fluctuates within a small range above and below the zero change.

(2) The overall change of differential settlement of the roadbed of the downstream line is small, with the maximum cumulative change of -0.938mm, and the cumulative change of each monitoring point does not exceed the warning value (±1.5mm). The cumulative change is roughly distributed in wave shape along the mileage, and the cumulative change of each monitoring point fluctuates within a small range above and below the zero change.

IV. B. 4) Comparison of manual reviews

Although the results of the automated monitoring data of the measuring robot basically coincide with the construction conditions, in order to assess the accuracy of the automated monitoring data of the measuring robot in various aspects, this project adopts the manual measurement method to review the automated monitoring data on a regular basis, and at the same time calibrate the stability of the reference network. Take a certain time upstream line and downstream line review results for analysis and research, the manual monitoring and automated monitoring data for difference comparison, manual review comparison results shown in Figure 7.

As can be seen from the figure, the measurement robot automated monitoring data and manual review results of the difference is relatively small, the difference between the two is generally located within ± 0.01mm, to manual review data as the reference value, to automated monitoring data for the measurement value, can be derived from the upstream line monitoring point of the tunnel bed settlement data error of 0.002mm, downstream line monitoring point of the tunnel bed settlement data error of 0.001mm. Therefore, using the underground environment monitoring system designed in this paper can realize the automated monitoring of the measurement robot, and its monitoring results and manual review of the data with a high degree of consistency, the automated monitoring data is more reliable, to meet the safety monitoring requirements of the tunnel bed settlement and deformation of long tunnels, and better ensure the safety of the construction of long tunnels.

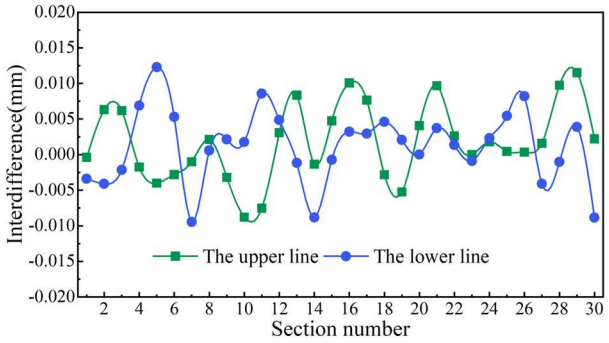

Figure 7: The comparison results of the manual review

IV. C. Gas Forecast Early Warning Analysis

IV. C. 1) Gas prediction model testing

Since the order of the gas concentration concentration prediction model and the parameters of the model are obtained by the estimation method, there is bound to be a certain deviation in the process, so before applying the established prediction model for gas concentration prediction, it is necessary to diagnose the established model and evaluate whether the deviation of the prediction model is in line with the prediction requirements. The relevant formula of ARIMA is utilized to fit the gas concentration of extra-long tunnels, and the fitting results are shown in Fig. 8. As can be seen from the figure, the ARIMA prediction model designed in this paper fits well with the historical monitoring data of tunnel gas concentration, and the maximum error between the fitted gas concentration data and the historical data does not exceed 0.5%. Therefore, it shows that the ARIMA model applied to the prediction of gas concentration in tunnels is feasible and can obtain more accurate gas concentration prediction results.

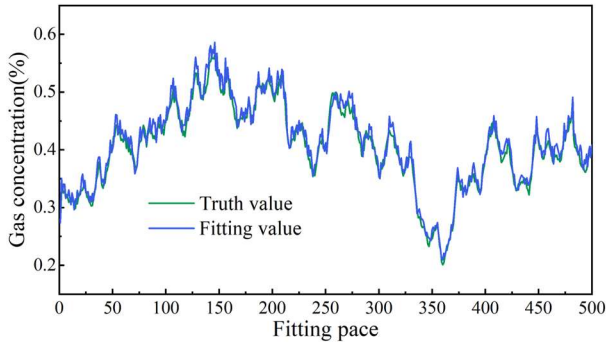

Figure 8: The actual value of the gas concentration is compared to the fitting value

Based on the formula for calculating the residual series of ARIMA simulation, the standard residual distribution of the residual series is obtained as shown in Figure 9. According to the outlier criterion for the standard residuals, the critical value is 2.25, so the negative standard residuals, which appear to be relatively large in absolute value in the figure, are not outliers. From the standard residual plot, it can be seen that the process does not have any tendency to change and fluctuates up and down around the 0 level line, i.e., it can be assumed that the process has a zero-mean and that the process contains all frequencies equally. Therefore, it can be assumed that the standard residuals of the gas concentration prediction model are consistent with the relevant properties of the white noise process, and the white noise test is passed, so the gas concentration prediction model ARIMA can roughly reflect the trend of the stochastic process of gas concentration.

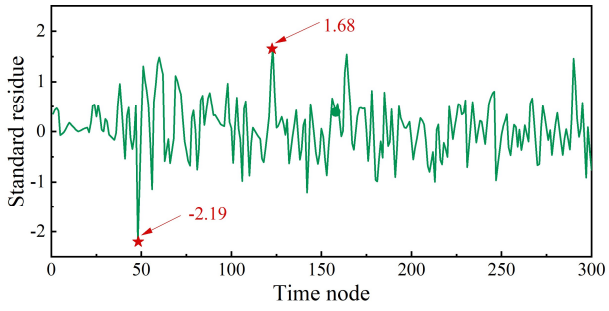

Figure 9: Standard residual map of the ARIMA model

The normality test is then performed on the standard residuals of the ARIMA model, where the quantile-quantile plot is used to test the normality of the standard residuals of the model. Figure 10 shows the Q-Q plot of the standard residuals of the ARIMA model. From the quantile-quantile plot of the standard residuals of the ARIMA model, it can be seen that except for a special outlier value at the beginning end point, the other points look very close to a straight line, especially the middle part and the extreme values almost coincide with the straight line, and this plot leads us to accept the assumption that the error term of the gas concentration prediction model ARIMA is normally distributed, i.e., the model developed is reasonable.

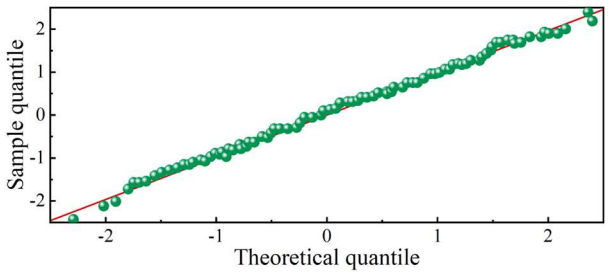

Figure 10: Standard residual and difference Q-Q diagram of the ARIMA model

Finally, to test the autocorrelation of the standardized residuals of the gas concentration prediction model, the sample ACF plots of the stochastic process of the residuals of the ARIMA model of the gas concentration prediction model are firstly plotted. In addition, in order to analyze whether the fitted residuals of ARIMA are new interest terms independent of the stochastic process, the Ljung-Box method is used in this paper for the test. Figure 11 shows the autocorrelation test results of the standardized residuals, where Figures 11(a)~(b) show the sample ACF plot and the Ljung-Box test results, respectively.

From the observation in the figure, it can be learned that the autocorrelation function value of the residual sample of the gas concentration prediction model is approximately 0, except for the slightly significant autocorrelation function value at the 12th-order lag, the other autocorrelation function values are not significant, thus, it can be considered that there is no autocorrelation in the residuals of the time-series prediction model of the gas concentration, ARIMA, and that the established gas concentration prediction model is reasonable. And the p-values of the test results are much larger than 0.01, so it can be concluded that the fitted residuals of the ARIMA model are new interest terms independent of the stochastic process itself, and the test of the gas concentration prediction model ARIMA passes without any modification, and it can be used directly for the prediction of gas concentration.

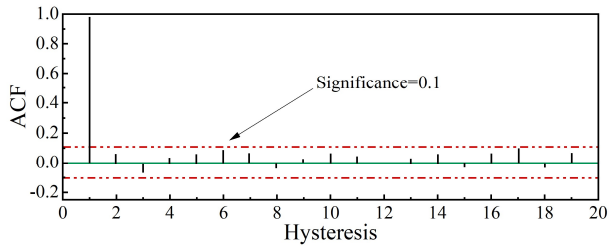

(a) Sample ACF of standard residual

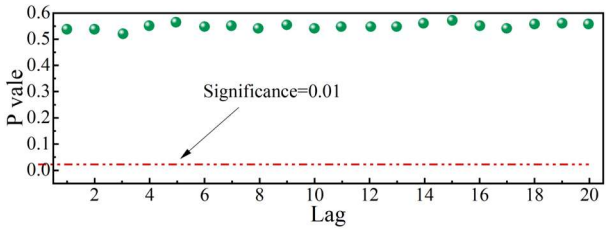

(b) Ljung-Box test results

Figure 11: Standard residual self-correlation test results

IV. C. 2) Trend prediction of gas concentration

The historical data of gas concentration in GQ tunnel is used as training to get the optimal ARIMA prediction model. The gas concentration after the excavation of the palm face on December 20, 2023 is predicted, and its prediction results are shown in Fig. 12, where Figs. 12(a)~(b) show the prediction results of the gas concentration as well as the prediction error, respectively.

As can be seen from the figure, the prediction error between the predicted data and the expected data is between -0.05% and 0.05%, and the relative error is between -8.02% and 9.57%. The prediction errors of gas concentration exceeding 0.045% include the three predicted values of 3rd, 22nd and 23rd, with values of -0.046%, 0.048% and 0.049%, respectively, but the relative errors of these three points are only -8.02%, 6.71% and 6.58%. Since the true values of gas concentration at these three points are relatively large, the existence of the above prediction errors is acceptable. Overall, the results of this gas concentration prediction are acceptable. From the gas concentration prediction results and errors of the underground environment of the tunnel on December 20, 2023, it can be seen that the maximum error of the gas concentration prediction is not more than 0.05%, and the relative error is not more than 9.57%, and the results of the gas concentration prediction of the underground environment of the extra-long tunnels by using the ARIMA model performs well.

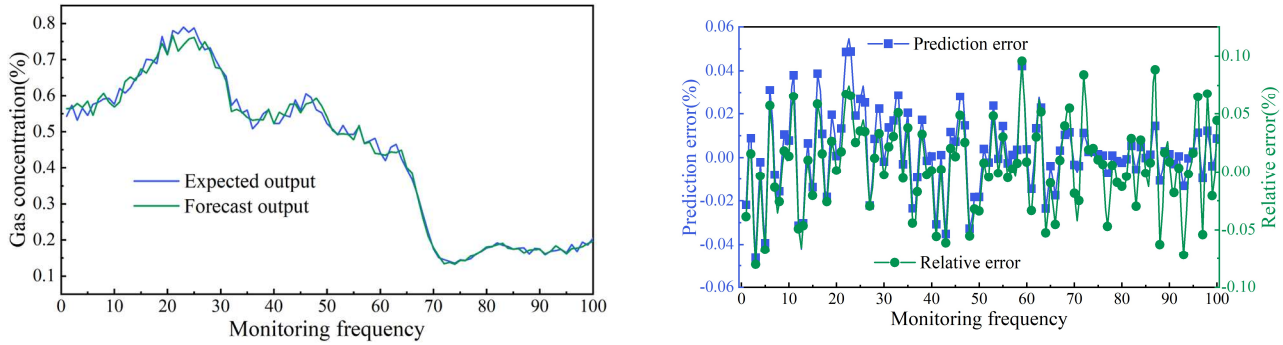

(a) Gas concentration prediction

(b) Gas concentration prediction error

Figure 12: Gas concentration trend prediction

IV. C. 3) Early warning analysis of gas concentration

Based on the example analysis of the gas concentration prediction model in Section 4.3.2, the ARIMA-based gas concentration prediction model is used to predict and analyze the gas concentration at the working face and the gas concentration at the upper corner of the GQ tunnel for early warning, respectively. The gas concentration sequences of five monitoring points from 09:00, December 20, 2023 to 09:00, December 26, 2023 are selected, with a time interval of 1 minute between each sample point, and each sample sequence contains 100 pieces of data. The first 80% of the gas concentration sample sequences are used as a training set for model training, and the last 20% of the gas concentration data are used as a test set, and finally the warning analysis is done based on the prediction results.

The mean value of the gas concentration monitoring sequence at the working face was 0.427, the variance was 0.022, and the confidence interval of 85% to 95% for the gas concentration was [0.452,0.463] according to the method of determining the threshold value of the gas concentration proposed in the previous section. When the predicted value of gas concentration is between [0.452,0.463] and the time of continuous increase is more than 10 minutes, then the gas concentration of the working face is judged to be a level Ⅰ warning. If the predicted value of gas concentration is greater than 0.463 and the time of continuous increase is more than 20 minutes, then it is judged to be class Ⅱ warning. Figure 13 shows the result of the working face gas concentration warning.

The analysis shows that at sample point 206, the predicted value of gas concentration is between [0.452,0.463], which is within the confidence interval of 85% to 95%, but the duration of increasing gas concentration is not more than 10 minutes, so it is in a safe condition, and there is no need to make a warning prompt. At sample points 151 through 156, the predicted values of gas concentration were between [0.452,0.463] with an interval of 1 minute between each sample point, so the increase in gas concentration lasted 5 minutes and was in a safe condition. At sample points 252 through 258, the predicted values of gas concentration were between [0.452,0.463], and the time of gas concentration increase lasted for 6 minutes and was in a safe condition. All other moments of the gas concentration values are in a safe state. According to the comparative analysis, it can be seen that the warning situation of the actual value is basically consistent with the warning situation of the predicted value. Therefore, the gas prediction and early warning of long tunnels based on ARIMA model has a better effect, realizes the gas early warning of the underground environment of long tunnels under the condition of guaranteeing the prediction accuracy, and better guarantees the safety in the construction process of long tunnels.

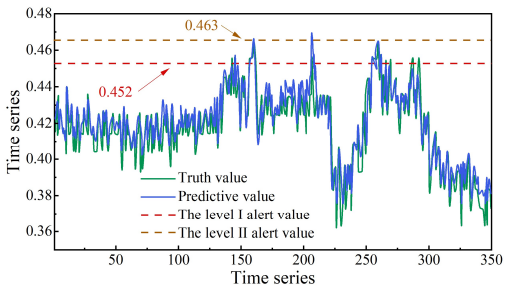

Figure 13: Early warning of the exposure of the face gas

V. Conclusion

The article proposes a system applied to the automatic monitoring of underground environment in very long tunnels, mainly for early warning monitoring of tunnel settlement and deformation and gas leakage. In order to verify the practicality of the underground environment intelligent monitoring system, the quantitative analysis of data is carried out by taking GQ tunnel as an example. The conclusions are as follows:

(1) Using the monitoring system designed in this paper for tunnel deformation and settlement monitoring, the average value of the deviation of X, Y and H coordinates of each measuring station and the error in the coordinates are all within 1mm, and the difference between the automated monitoring data and the manual review results is relatively small, and the difference is generally located in the range of ±0.01mm. Therefore, the use of underground environment monitoring system of long tunnels can realize real-time monitoring of tunnel bed settlement and deformation, and provide reliable data support for optimizing the tunnel construction plan.

(2) Before the gas early warning, the trend of gas concentration is predicted by ARIMA model, and the prediction error between its predicted data and expected data is between -0.05% and 0.05%. Combined with the interval changes of the time series at different points, the graded warning of gas concentration can be realized to effectively improve the safety performance of tunnel construction.

Funding

This work was supported by CCCG.

References

[1] Liu, X., Fang, Q., Zhang, D., & Wang, Z. (2019). Behaviour of existing tunnel due to new tunnel construction below. Computers and Geotechnics, 110, 71-81.
[2] Chapman, D. N., Metje, N., & Stark, A. (2017). Introduction to tunnel construction. Crc Press.
[3] Ye, F., Qin, N., Liang, X., Ouyang, A., Qin, Z., & Su, E. (2021). Analyses of the defects in highway tunnels in China. Tunnelling and Underground Space Technology, 107, 103658.
[4] Moretti, L., Cantisani, G., & Di Mascio, P. (2016). Management of road tunnels: Construction, maintenance and lighting costs. Tunnelling and Underground Space Technology, 51, 84-89.
[5] Zhang, Y., & Li, X. (2020). Monitoring and analysis of subway tunnel thermal environment: A case study in Guangzhou, China. Sustainable Cities and Society, 55, 102057.
[6] Hsu, W. L., Ouyang, Z., Dong, Z., Wu, F., Chiu, C. Y., & Liarng, R. H. (2022). Evaluation of Procurement of Environment Monitoring Equipment for Tunnel Construction. Sensors & Materials, 34.
[7] Liu, R., He, Y., Zhao, Y., Jiang, X., & Ren, S. (2020). Tunnel construction ventilation frequency-control based on radial basis function neural network. Automation in Construction, 118, 103293.
[8] Liu, J. Q., Sun, Y. K., Li, C. J., Yuan, H. L., Chen, W. Z., Liu, X. Y., & Zhou, X. S. (2022). Field monitoring and numerical analysis of tunnel water inrush and the environmental changes. Tunnelling and Underground Space Technology, 122, 104360.
[9] Zhang, F., & Hu, B. (2024). Design and Application of Microcontroller-Based Tunnel Construction Environment Monitor. Tehnički vjesnik, 31(4), 1060-1068.
[10] Park, W. H., Cho, Y., & Kwon, T. S. (2016). Development of Tunnel-Environment Monitoring System and Its Installation III-Measurement in Solan Tunnel. Journal of the Korea Academia-Industrial cooperation Society, 17(5), 637-644.
[11] Jiang, H., Huang, H., Lu, C., & Yang, T. (2024). Design and Application of Tunnel Service Safety Monitoring and Early Warning System Based on Multi-Sensor. In Mechatronics and Automation Technology (pp. 619-627). IOS Press.
[12] Qiu, D., Qu, C., Xue, Y., Zhou, B., Li, X., Ma, X., & Cui, J. (2020). A Comprehensive Assessment Method for Safety Risk of Gas Tunnel Construction Based on Fuzzy Bayesian Network. Polish Journal of Environmental Studies, 29(6).
[13] Guo, C., Xu, J., Yang, L., Guo, X., Liao, J., Zheng, X., ... & Wang, M. (2019). Life cycle evaluation of greenhouse gas emissions of a highway tunnel: A case study in China. Journal of cleaner production, 211, 972-980.
[14] Li, Z., Wu, J., Liu, M., Li, Y., & Ma, Q. (2019). Numerical analysis of the characteristics of gas explosion process in natural gas compartment of utility tunnel using FLACS. Sustainability, 12(1), 153.
[15] Xue, Y., Chen, G., Zhang, Q., Xie, M., & Ma, J. (2021). Simulation of the dynamic response of an urban utility tunnel under a natural gas explosion. Tunnelling and Underground Space Technology, 108, 103713.
[16] Chen, D., Wu, C., Li, J., & Liao, K. (2022). A numerical study of gas explosion with progressive venting in a utility tunnel. Process Safety and Environmental Protection, 162, 1124-1138.
[17] Weerheijm, J., Verreault, J., & Van Der Voort, M. M. (2018). Quantitative risk analysis of gas explosions in tunnels. Fire Safety Journal, 97, 146-158.
[18] Chen, D., Zhang, H., Li, J., Liu, K., Wang, Y., Huang, Y., ... & Wu, C. (2024). A full-scale experimental investigation of natural gas explosion in a 710-m long utility tunnel with multiple pipelines. Tunnelling and Underground Space Technology, 153, 106049.
[19] Zhang, P., Lan, H. Q., & Yu, M. (2021). Reliability evaluation for ventilation system of gas tunnel based on Bayesian network. Tunnelling and Underground Space Technology, 112, 103882.
[20] Zhu, G., Zhao, H., Liu, Z., & Shi, C. (2020). Design and Implementation of Tunnel Environment Monitoring System Based on LoRa. In IoT as a Service: 5th EAI International Conference, IoTaaS 2019, Xi'an, China, November 16-17, 2019, Proceedings 5 (pp. 621-638). Springer International Publishing.

[21] Wan, L., Zhang, C., Chen, G., Zhou, Y., Zhang, X., & Tao, C. (2022, November). Design and simulation of tunnel real-time monitoring system based on multivariate information fusion. In International Conference on Frontiers of Traffic and Transportation Engineering (FTTE 2022) (Vol. 12340, pp. 56-63). SPIE.
[22] Sun Xiaoming,Zhu Jiajie,Xu Yongzhen,Ren Chao,Yang Kai,Zhang Fujun... & Yuan Junchao. (2021). Multisource monitoring and early warning system of rock burst in the Gaoloushan deep-buried tunnel. IOP Conference Series: Earth and Environmental Science(4).
[23] Zhang Yu,Zhong Ruofei,Li Yongrong & Sun Haili. (2021). Research on Monitoring Method of Remote Deformation and System Application Based on Image. Advances in Civil Engineering.
[24] BaumannOuyang Andreas,Butt Jemil Avers,Varga Matej & Wieser Andreas. (2023). MIMO-SAR Interferometric Measurements for Wind Turbine Tower Deformation Monitoring. Energies(3),1518-1518.
[25] Guo Yanwei,Li Xiongwei,Ju Shangwei,Lyu Qifeng & Liu Tao. (2022). Utilization of 3D Laser Scanning for Stability Evaluation and Deformation Monitoring of Landslides. Journal of Environmental and Public Health8225322-8225322.
[26] Li Chuan,Fang Xinqiu,Yan Zhenguo,Huang Yuxin & Liang Minfu. (2023). Research on Gas Concentration Prediction Based on the ARIMA-LSTM Combination Model. Processes(1),174-174.